Jurnal Teknologi

Full Paper

# MODIFICATION OF NANO HYBRID PES-ZNO MEMBRANE USING UV IRRADIATION FOR BIODIESEL PURIFICATION

Tutuk Djoko Kusworo[a,b]*, Andri Cahyo Kumoro[a], Muhammad Ainul Yaqin[a], Nurul Fatiyah[a], Dani Puji Utomo[a]

[a]Chemical Engineering Department, Faculty of Engineering, Universitas Diponegoro, Semarang, Indonesia
[b]Membrane Research Center (Mer-C), Universitas Diponegoro, Semarang, Indonesia

**Article history**
Received
*20 February 2020*
Received in revised form
*3 August 2020*
Accepted
*9 August 2020*
Published online
*27 August 2020*

*Corresponding author
tdkusworo@che.undip.ac.id

## Graphical abstract

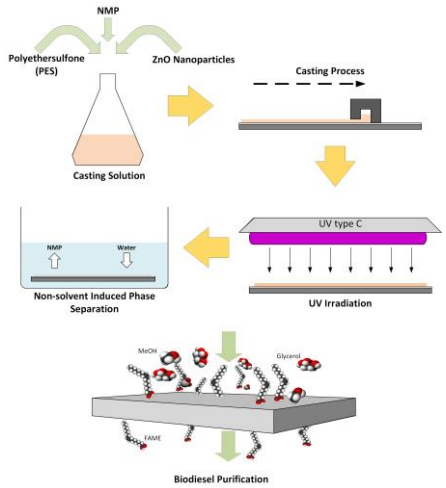


## Abstract

The purification of biodiesel is one of the crucial processes involved in biodiesel production. This study aims to examine the effect of the polymer composition, nano-ZnO loading, and UV irradiation on the performance of membranes for biodiesel purification. The membranes were fabricated with the polyethersulfone composition of 17, 18, and 20 wt%. The compositions of nano ZnO were varied at 1.5, 2, and 2.5 wt%, while the duration of UV irradiation was varied for 0.5, 1, and 1.5 minutes. The results indicate that the compositions of PES, nano ZnO, and UV irradiation affected the performance of the membrane. The best membrane performance was achieved when the membrane was produced using PES 17 wt%, nano ZnO 1.5 wt% involving irradiation UV light for 1 minute. The fabricated membrane exhibits 3 hours flux profile stability and 61.5% glycerol rejection.

*Keywords*: Purification, Biodiesel, Membrane, PES-ZnO, UV irradiation



## 1.0 INTRODUCTION

Industrial development in Indonesia has led to a significant increase in the consumption of fossil-based fuels. According to the BP Statistical Review of World Energy [1], Indonesia consumed 1,615 million barrels of crude oil every day in 2017. Besides, extensive exploration and uses of fossil fuels potentially harm the ecosystem. According to Brennan and Owende [2], in 2006, fossil fuels contributed approximately 29 billion tons of the world's $CO_2$ emissions. The emitted $CO_2$ can be absorbed by the ocean, which leads to alter the pH of the seawater and trigger the decline of marine life quality. Therefore, alternative renewable energy sources are required to substitute fossil-based fuels, especially those derived from natural resources. Biodiesel is an alternative fuel for diesel engine, which is commonly produced by transesterification reactions of vegetable oils, animal fats or their combination to produce fatty acid methyl esters (FAME) [3], [4]. Unfortunately, transesterification reactions produce by-products, such as glycerol, soap, residual triglycerides, diglycerides, monoglycerides, catalysts, water, and solvents [5]. Also, the production of biodiesel with a transesterification reaction requires subsequent purification processes.

Many researchers have carried out various studies related to biodiesel purifications. Alves *et al*. [6] conducted biodiesel purification employing the adsorption process using bagasse as adsorbent. Although this study has successfully reduced the

water content to 600-1200 ppm, this value is still higher than the standard of moisture content, which is 500 ppm (EN 14213). Besides, the amount of biodiesel produced decreases to about 8-10 wt%. In another study, Wall *et al*. [7] used ion exchange resins to purify biodiesel. This study requires an additional cost to use resin. They also found a correlation between the type of resin with the purified biodiesel. Escorsim *et al*. [8] used pressurized $CO_2$ (6-12 MPa) to adsorb impurities in biodiesel for purification purposes at 298-323K. Even though this method resulted in purity biodiesel (higher than 90%), but this method requires a very high amount of $CO_2$, which is 50% of the total weight of crude biodiesel. Alves [9] used *polyethersulfone* ultrafiltration membrane technology to purify biodiesel. They also reported that the moisture of the biodiesel was 1026.2 ppm, which was still higher than the international standard. Atadashi [10] examined the purification of biodiesel using a sequential method, which comprised the dry washing method and followed by polyacrylonitrile (PAN) membrane separation to produce biodiesel with a residual glycerol concentration of 0.007 wt%. However, the use of the PAN membrane for biodiesel purification suffered many disadvantages. One of them being the short membrane's life span due to high solvent concentration in the PAN solution. To overcome the fouling problem encountered in the membrane applications involving organic substances, many researches has focused on the fabrication of functional membranes with considerable antifouling properties through the improvement of membrane's surface hydrophilicity [11]. Shen [12] examined the characteristics of PES/ZnO membranes and found that the addition of ZnO to the membrane increases water permeability as a result of increasing membrane porosity, rejection and subsequently decreases the fouling of the membrane surfaces.

In this study, the PES-ZnO membrane Nanohybrid was developed for biodiesel refining. The PES-ZnO membrane nanohybrids used in this study underwent surface modification to improve the antifouling properties. This research examined the effect of PES and ZnO compositions in the doping solution and the duration of UV irradiation on PES–ZnO membrane performances for refining biodiesel.

## 2.0 METHODOLOGY

### Materials

The polyethersulfone (PES) Veradel® PESU 3100P was purchased from Solvay Advanced Material (USA). Nano ZnO and N-Methyl-2-Pyrrolidine (NMP) were obtained from Nano Center Indonesia (Tangerang, Indonesia) and Merck KgaA (Germany), respectively. The crude biodiesel was obtained from Artha Metro Oil, Ltd. (Sidoarjo, Indonesia) with the characteristics presented in Table 1.

**Table 1** Characteristics of crude biodiesel

| Parameter | Value |
|---|---|
| Density 15°C, $g.L^{-1}$ | 889.5 |
| Water content, wt.% | 0.08 |
| Acid Value, $mg\text{-}KOH.g^{-1}$ | 0.42 |
| Glycerol, wt.% | 3.98 |
| Kinematic Viscosity at 40°C, $mm^2.s^{-1}$ | 4.00 |

### Membrane Fabrication

In this study, membrane fabrication was carried out through three stages. First, the membrane solution was prepared by dissolving polyethersulfone (PES) polymer membranes with compositions of 17, 18, and 20% weight in N-Methyl-2Pyrrolidine (NMP). The solution was then mixed for 8 hours, and the doping solution was left for 24 hours for air bubbles removal. The membrane was then cast using a phase inversion technique by pouring the doping solution over a glass plate. The casting knife was sheared to on the glass plate to obtain a thin sheet membrane. Then the thin sheet membrane was immersed in a coagulant bath and left for 24 hours before further removed by non-solvent. Then the membrane was dried for 24 hours, and the flux test was performed by using dead-end cell filtration, as shown in Figure 1. The best membrane sheets were applied to the next stage.

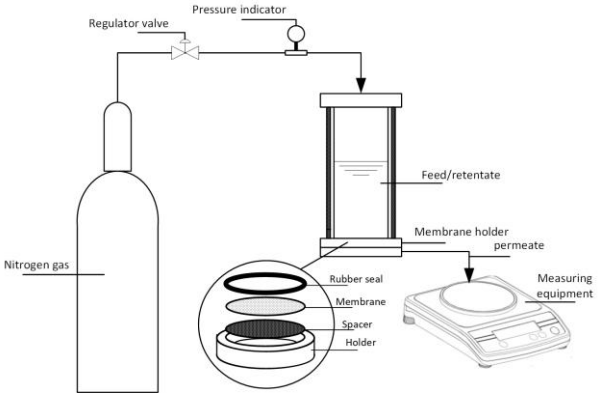


**Figure 1** Schematic diagram of the dead-end cell filtration set-up

Upon the achievement of the best PES composition, the next step was fabricating membrane with nano ZnO as filler with a composition of 1, 2, and 2.5% total solids. This process was conducted by mixing nano ZnO into a doping solution. The ZnO should be dissolved in NMP with the help of ultrasonication to avoid the formation of ZnO aggregates to ensure complete mixing with the PES doping solution. Similar to the previous stage, the homogeneous doping solution was cast to obtain membrane sheets and tested using dead-end filtration cells. The best ZnO composition obtained was used for the next stage.

The next step was to fabricate a membrane with ultraviolet (UV) irradiation. This process was carried out by preparing a doping solution containing PES and nano ZnO mixture. After the doping solution was cast, the obtained membrane sheet was subjected to UV irradiation for 0.5, 1, 1.5 minutes. Then the membrane was immersed into the coagulant. Furthermore, the membrane was tested using dead-end filtration cells. The membrane performances were evaluated to obtain the best irradiation time. The fabricated membrane formulas in this study are resumed in Table 2.

**Table 2** List of doping solution formula and modification treatment

| Membrane | PES (wt-%) | Nano ZnO (wt-%) | NMP (wt-%) | UV irradiation (minute) |
|---|---|---|---|---|
| M1 | 17 | - | 83 | - |
| M2 | 18 | - | 82 | - |
| M3 | 20 | - | 80 | - |
| M4 | 17 | 1.5 | 81.5 | - |
| M5 | 17 | 2 | 81 | - |
| M6 | 17 | 2.5 | 80.5 | - |
| M7 | 17 | 1.5 | 81.5 | 0.5 |
| M8 | 17 | 1.5 | 81.5 | 1 |
| M9 | 17 | 1.5 | 81.5 | 1.5 |

## Biodiesel Purification Experiment

The flux value of the membrane was determined using the dead-end filtration cells test. In the filtration cells, filter support and membrane were placed in a membrane holder for the permeability test. The filtration vessel was filled with biodiesel and closed hermetically. The permeability flux was obtained by measuring the mass of biodiesel every 45 minutes. Flux values were calculated by calculating the ratio of permeate volume per unit of membrane area per unit time, as expressed in Equation (1).

$$J = \frac{\Delta m}{A.\Delta t} \quad (1)$$

Where J ($kg.m^{-2}.h^{-1}$) is permeate flux, Δm (kg) is the mass of collected permeate during the time interval Δt (h), and A (0.0015 $m^2$) is the effective membrane area.

Rejection coefficient was calculated by determining the glycerol concentration of feed and filtered biodiesel. The permeate was used to determine the glycerol content remaining in the biodiesel. For determining total glycerol content in the biodiesel, the proposed method by Pisarello [13] was employed. Pisarello has compared his proposed method with the standard method using GC analysis based on ASTM and EN Standards. The difference between them wasn't quite significant. The proposed method doesn't have any raw material limitation, while the GC analysis does have.

$$C_{gly} = \frac{\Delta V_i N_i MW_{gly}}{1000 \times m} \times 100\% \quad (2)$$

Where $C_{gly}$ (%) is glycerol content in biodiesel, $\Delta V_i$ (mL) and $N_i$ ($mol_{eq}/L$) are volume and normality of titrant, respectively. $MW_{gly}$ (92.0938 g/mol) is the molecular weight of glycerol, m (g) is sample mass. Glycerol rejection can be calculated using Equation 3.

$$R = 1 - \frac{C_p}{C_f} \quad (3)$$

where R is rejection efficiency, $C_p$ and $C_f$ are the concentration of glycerol in permeate and feed, respectively.

Field emission scanning electron microscopy (FESEM) was used to determine the dimension of the fibers. Membrane samples were fractured in liquid nitrogen. They were then mounted on an aluminum disk with a double surface tape with the sample holder was placed and evacuated in a sputter-coater with gold.

## Porosity and Pore Radius Assessment of Membrane

Membrane porosity was measured using the dry-wet weight method following the procedure previously applied by Liao *et al*. [14]. Porosity ε (%) of the membrane was determined according to Equation 4.

$$\varepsilon = \frac{(W_1 - W_2)/\rho_{water}}{(W_1 - W_2)/\rho_{water} - W_2/\rho_{PES}} \quad (4)$$

Where $W_1$ is the wet sample weight, $W_2$ is the dry sample weight, $\rho_{water}$ is the density of pure water at 25°C ($kg/m^3$), and $\rho_{PES}$ is the density of dry state membrane ($kg/m^3$). Subsequently, the average pore size $r_m$ (m) was determined by the filtration velocity method. According to Guerout-Elford-Ferry Equation, $r_m$ can be calculated using Equation 5.

$$r_m = \sqrt{\frac{(2.9 - 1.7\varepsilon) \times 8 \times \eta \times l \times Q_t}{\varepsilon \times A \times \Delta P}} \quad (5)$$

Where, η was the biodiesel viscosity at 25°C, *l* is the membrane thickness(m), $Q_t$ is the permeate volume biodiesel per unit of time($m^3/h$), *A* is the effective area pf the membrane($m^2$), and ΔP is the operational pressure (MPa).

### Membrane Characterization Using Fourier Transform Infrared Spectroscopy

Membrane characterization using FTIR was performed to determine the functional groups that exist in the membrane matrix that may change as a result of the modification. Transmittance values at specific wavelengths indicate the presence of functional groups in the membrane [15].

### Membrane Characterization Using Scanning Electron Microscope

The determination of membrane morphology was carried out by Scanning Electron Microscopy (SEM) method. First, the membrane was dried at 40°C. To analyze the surface morphology of the membrane, dry samples were placed above the preparation site. To analyze the morphology of the cross-section of the membrane, the sample was fractured down in liquid nitrogen. Before the image was taken, the membrane was lifted and fractured with both tweezers. This piece of the membrane was coated with pure gold (coating), which serves as a conduit. Furthermore, cross-sections and membrane surfaces are photographed with selected magnifications [16].

### Water Contact Angle Measurement

Contact angle analysis was done by using Race Angle Meter with ion-free distilled water at 25°C. This analysis aims to characterize the membranes, whether they are hydrophilic or hydrophobic. If the contact angle is greater than 90°, the membrane is considered as hydrophobic with poor adhesiveness, poor wettability, and low free energy of solid surfaces. Meanwhile, a membrane with a contact angle of less than 90° indicates that the membrane is hydrophilic, which demonstrates excellent adhesion, good wettability, and high free energy of solid surfaces [17]. In this analysis, measurements were made at three points on the left and right sides of the membrane.

## 3.0 RESULTS AND DISCUSSION

### The Effect of PES Concentration on PES Membrane Performance

Biodiesel filtration using a dead-end system was performed to assess the permeability and selectivity of the PES-Nano ZnO membrane. The system was operated at 4 bar for 3 hours. The permeate samples were taken every 45 minutes to determine its permeability and glycerol content.

Figure 2 shows the permeate profile for various PES concentrations used in the membrane fabrications. For all membranes, the flux decreases as the filtration proceeds. The flux achieved by each membrane decreases along with the increase of the PES concentration used in the membrane. The membrane with 17 wt% PES has a dramatic flux decrease compared to the other membranes, while membranes with 18 wt% and 20 %wt PES exhibit more stable flux.

Decreasing flux obtained as time function is probably caused by the accumulation of rejected glycerol and impurities. This accumulation increase as the filtration goes by, leading to a decrease in the pore size in membranes and subsequently reduce the flux [18]. Membrane with PES 17 wt% has a significant drop compared to other membranes. Usually, a membrane with less PES concentration exhibit lower tensile strength. As a result, at a given operating pressure, a membrane with less PES content will be more compact than those with higher PES content, which in turn leads to a more pronounced flux reduction.

As mentioned earlier, the increasing of initial polymer concentration leads to the achievement of higher flux. To discuss this phenomenon, an investigation of the effect of polymer concentration on membrane porosity is required. Figure 2 (c) shows that an increase in polymer used decreases the pore size of the membranes. An increase in PES used will consequently reduce the solvent used. As a result, the void space formed in the membrane upon immersion in the coagulation bath decreases and leads to decreasing pore size. Finally, the decrease of pore size leads to a decrease in the permeability of the membrane for filtration purposes [19].

Figure 2 (b) shows that increasing PES content in the membranes increases the total glycerol rejection. Three factors can influence the rejection in the membrane filtration process, namely ion charges on the surface of the membrane, hydrophilicity, and the effect of pore sieving [20]. PES concentrations do not significantly change the ion charge on the membrane surface because the membrane composition only consists of poly (ether sulfone) and N-methyl-2-pyrrolidone so that the electronegativity of the membrane tends to be stable. The ion load on the membrane surface only changes as the membrane is incorporated by nanofillers. The size of the membrane pore influences the pore sieving membrane's ability. The greater the PES concentration in the membrane, the smaller the pores formed [18]. Pores in membranes will affect the ability of membranes to select component components based on the size of membrane pore and the dissolved solute.

The polymer concentration in the membrane will also affect the hydrophilicity of the membrane. PES is a pure hydrophilic compound so that the higher the concentration of this polymer will cause the membrane to be more hydrophilic. Glycerol is highly soluble in water, so glycerol can be regarded to be hydrophilic when the hydrophilicity of the membrane increases; the quantity of the glycerol adsorbed on the membrane surface will increase. Adsorption of glycerol on the surface of the membrane will cause pore plugging so that it can increase the amount of

glycerol retained. Therefore, higher hydrophilicity of the membrane will cause a higher amount of retained glycerol due to pore sieving and membrane adsorption. This condition leads to a higher rejection rate of the membrane [19].

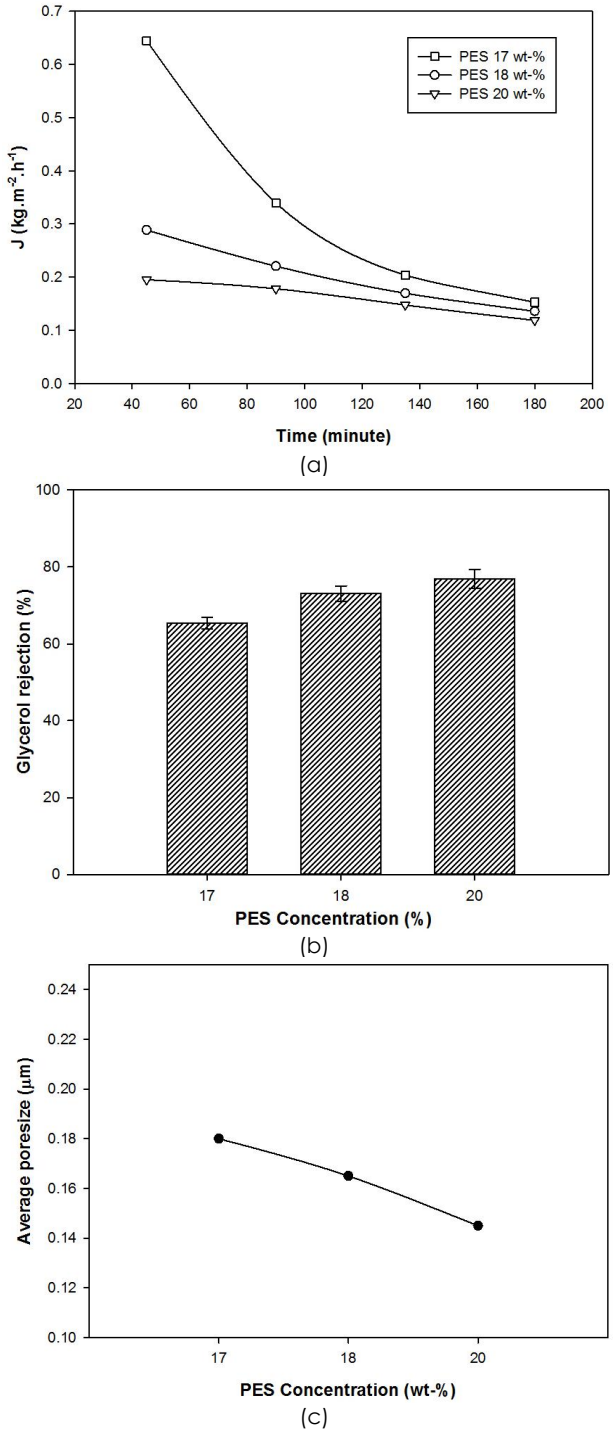


**Figure 2** The performance of membranes with various PES concentration used (a) Flux Profile (b) Total Glycerol Rejection (c) Pore Size

## The Effect of Nano ZnO Loading on Modified Nano ZnO-PES Membrane Performance

The flux of the membrane increases with increasing nano ZnO composition. However, the flux tends to decrease as time increases, as shown in Figure 3 (a). The increase in the flux of the nanohybrid membrane can be due to the formation of ZnO nano aggregate on the membrane surface, which leads to an increase in the membrane pore size [21]. The addition of nanoparticles promotes the solvents and non-solvents diffusion exchange when the doping solution immersed so the formed membrane resulting in a bigger pore size. This phenomenon is called instantaneous demixing [22]. Besides, there is an obvious flux difference between PES membranes with 1.5 wt% and 2.0 wt% Nano ZnO loadings. When less Nano ZnO used in the preparation of the membranes, the possibility of Nano ZnO aggregate formation is smaller. Membranes with 1.5 wt% Nano ZnO loading will promote a more uniform Nano ZnO particle distribution compared to the others. As explained before, the aggregates can interfere with the interaction among the polymer's molecules leading to smaller pore sizes. The decreasing tendency of the flux with time may the result of the accumulation of foul on the membrane's pore. The accumulation of foul will decrease the pore size and subsequently reduces the volume of the permeate and finally causes flux reduction [23].

Figure 3 (b) shows that the addition of nano ZnO decreases glycerol rejection. This phenomenon is caused by the increasing number and size of the membrane's pores, which leads to reduce the glycerol rejection [21].

From the previous research, [24] explained that the addition of nano ZnO would influence the separation mechanism so that membrane rejection will decrease. In addition, the addition of nano ZnO increase aggregates formed on the membrane surface, which affect the surface of the membrane becomes no longer homogeneous so that the membrane's performance will be different on each surface. This also causes the membrane's ability to hold particles to be different for each part.

Indeed, the use of nano ZnO influences the characteristics and performance of the membranes. Increasing of nano ZnO composition causes nano ZnO agglomeration in the membrane, which in turn reduces the hydroxyl group on the modified membrane surface [25].

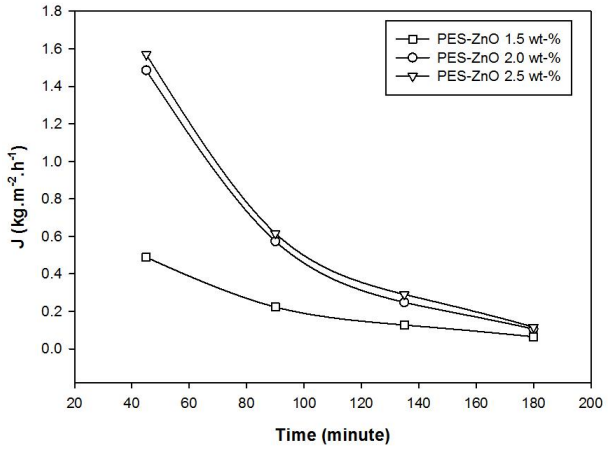


(a)

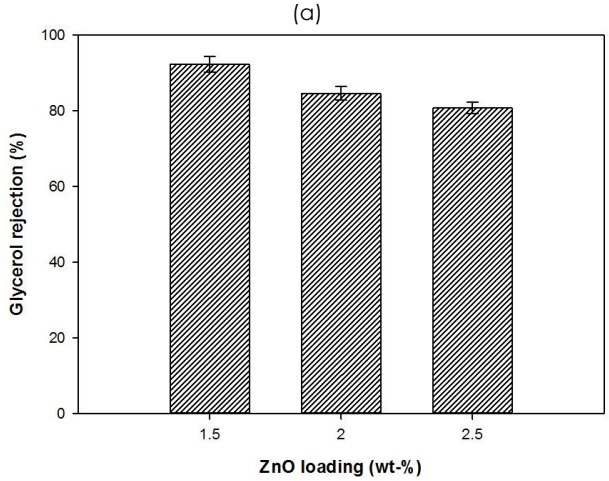


(b)

**Figure 3** Membrane performance with various Nano ZnO Loading (a) Flux profile (b)Total Glycerin Rejection

## The Effect of UV Irradiation Time on Membrane Performance

From Figure 4 (a), it can be seen that the flux of each UV irradiation time is relatively stable. The UV irradiation on the membrane for half a minute produced the highest flux and followed by UV irradiation for 1.5 minutes and 1 minute. UV irradiation causes an increase in flux compared to the membranes without UV irradiation (Figure 1 (a)). However, the flux profile shown by 0.5 min UV irradiated membrane exhibits an unusual phenomenon where the flux slightly increases beyond 90 min filtration. The possible answer is that the membrane experienced a slight reduction of its hydrophilic property due to short exposure to UV irradiation during the preparation. This result is in accordance with its higher contact angle with the membranes with longer exposure to UV irradiation, as seen in Table 3. This condition prompts the penetration followed with the attachment of FAME on the membrane pore walls that increases the affinity of the membrane with FAME molecules. As the membrane-FAME affinity increases, the flux profile increases with the consequences of lower glycerol rejection rate, as shown in Figure 4(b).

When viewed from the time of UV irradiation, there was a dramatic decrease in the flux of the membrane as it was UV irradiated for 0.5 minutes and 1 minute. However, the flux of the membrane increased when it was irradiated for 1.5 minutes. The decrease in the flux of the membrane is triggered by the time lag between the casting and immersion processes of the doping solution. The time lag causes some solvent to evaporate and undergo "delayed demixing". As a result, the membrane obtained is denser than the membrane obtained by the instantaneous demixing process, which leads to a decrease in the flux [19]. On the other hand, the increasing flux is caused UV irradiation starts to damage the polymer matrix [19] and cuts the polymer chains [26]. Both of these phenomena will enlarge the pores that are in the membrane.

Figure 4 (b) shows that the duration of UV irradiation affects the rejection of glycerol. Kusworo *et al*. [24] explained that UV irradiation causes membranes to experience chain scission and cross-linking. As a result, the membrane pore will be tightened and preventing more contaminants from being carried away by the permeate. In addition, the duration of irradiation can induce the degradation of the membrane polymer chains resulting in simpler compounds or a molecule's structure.

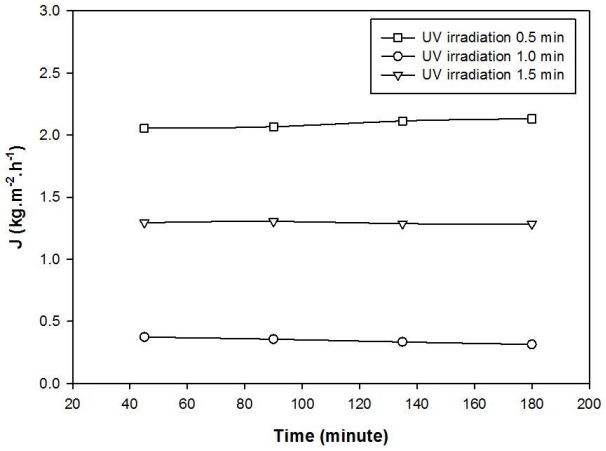


**(a)**

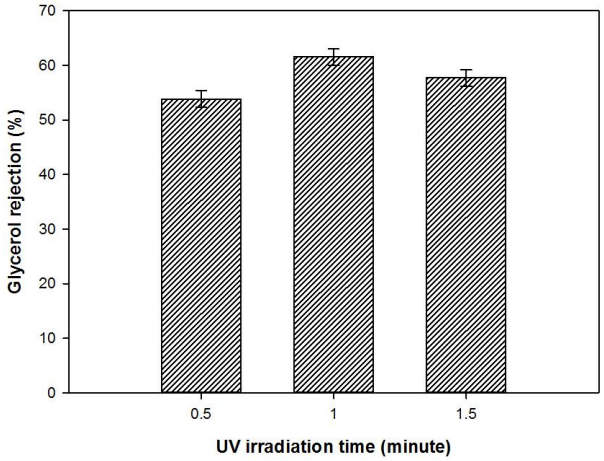


**(b)**

**Figure 4** Membrane performance with various UV irradiation time (a) Flux profile (b)Total Glycerin Rejection

## Membrane Characterization using Fourier Transform Infra-red (FTIR) Spectrophotometry

In this study, FTIR analysis of three membranes, namely PES 17% membrane, PES 17% -ZnO 1.5% membrane, and PES 17%-ZnO 1.5% - UV 1 min membrane to investigate the effect of ZnO nano addition and influence UV irradiation of membrane functional groups. The results are shown in Figure 5.

Based on Figure 5, the peaks of the three membranes were observed at frequencies 563, 840, 1150 -1240, 1485, 1578 and 1670 $cm^{-1}$ suggesting the existence of each metal-oxide functional group, Cis ZC=CZ, CO stretching vibration (for wavenumber of 1000-1300 $cm^{-1}$), trans RC = CR (for wavenumber 1400-1600 $cm^{-1}$) [27]. A noticeable difference can be observed in the range 1600 - 1700 $cm^{-1}$. The transmittance of the UV irradiated membrane at 1675 $cm^{-1}$, which belongs to carbonyl stretching, was higher than that of the neat membrane.

For bands 563 and 840, the peak of membranes with ZnO had lower transmittance that of pristine PES membrane, but for bands with a range of 1400-1600, peak of membranes with ZnO have higher transmittance that of the pristine membrane. This phenomenon is caused by the change in functional groups to Zn groups. So, the transmittance due to the Zn-C bond decreases, and the transmittance due to the R-C bond rises to the membrane with ZnO.

The weak peak at a wavenumber of 1707 $cm^{-1}$, which indicates the existence of RC=CR stretching, is disappearing in the spectra of UV irradiated membrane designating a change in RC=CR functional group structure that caused by the polymer chain breakdown caused by UV irradiation [28].

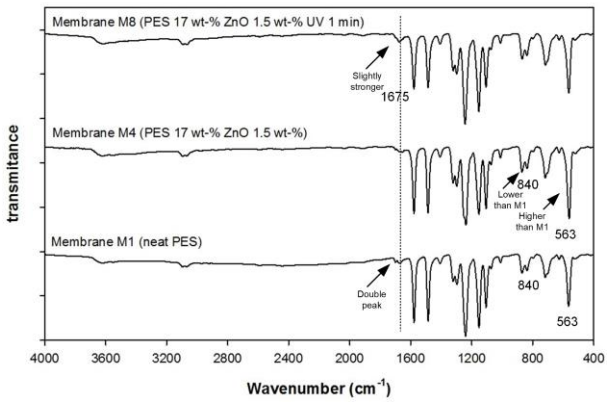


**Figure 5** FTIR Spectra of fabricated membranes

## Membrane Morphology Characterization using a Scanning Electron Microscope (SEM)

Surface and cross-section morphology of membranes are essential data to obtain the detail information of the membrane transport phenomena. The surface morphology of the membrane was performed by SEM at 200x magnification. There were three membranes analyzed on this analysis; PES 17 wt%, PES 17wt% ZnO 1.5wt%, Nano ZnO-PES with UV for 1 minute.

Figure 6 shows that the neat PES membrane exhibits a smoother surface and less void compared to the other membranes. Neat PES membrane consists of polymer and solvent as the results of the interaction between its polymer particles would not be interrupted by any means. Compared to the neat PES membrane, both modified membranes have more void space, especially the UV irradiated PES membrane. At some point, UV irradiation can damage the polymer interactions in membranes, resulting in a higher permeability. Even though UV irradiation has a side effect on membranes, the UV irradiation can induce better interactions between ZnO ion with polymer than those without UV irradiation. This phenomenon is proven, as seen in Figure 5B-1 and C-1. The surface of the membrane with UV irradiation has more uniformly distributed white spots than those of neat membranes. These white spots are supposed to be the ZnO particles.

The inorganic material is added to the doping solution to improve membrane performance. Inorganic material addition should be distributed more regularly in the dense layer as it will increase the membrane's permeability and rejection. Figure 6 B-2 shows the formation of some Nano ZnO aggregates. Aggregate formed in membranes interrupts the interaction between polymers as it can lose the pore size distribution. As a result, increasing permeability will not be followed by increasing rejection but decreasing it instead.

Figure 6 C-2 shows UV irradiation affects the membranes sheet layers. It shows that UV irradiation damages the dense layers and leads to increase the

permeability. In addition, UV light can also increase pore size. This is proven by the formation of a more finger-like porous structure than other membranes. Increasing porous structure in membranes by UV leads to less foulant accumulation in the membranes. As a result, the permeability of the UV irradiated membranes is more stable compared to other membranes.

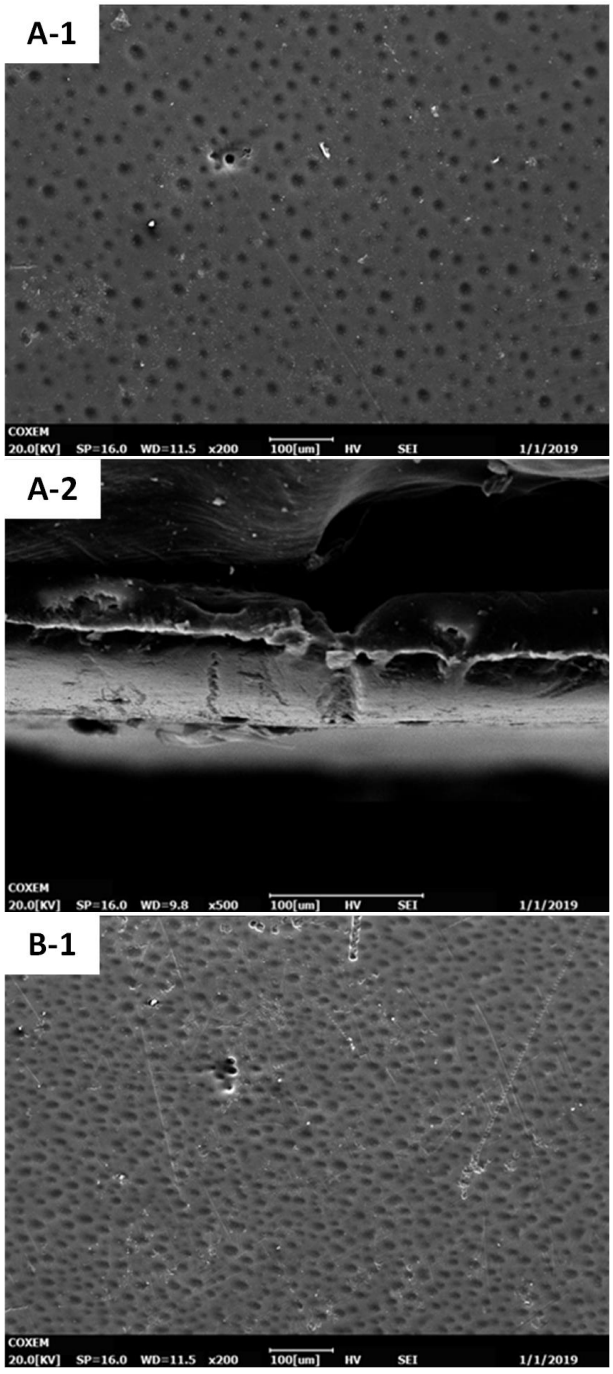


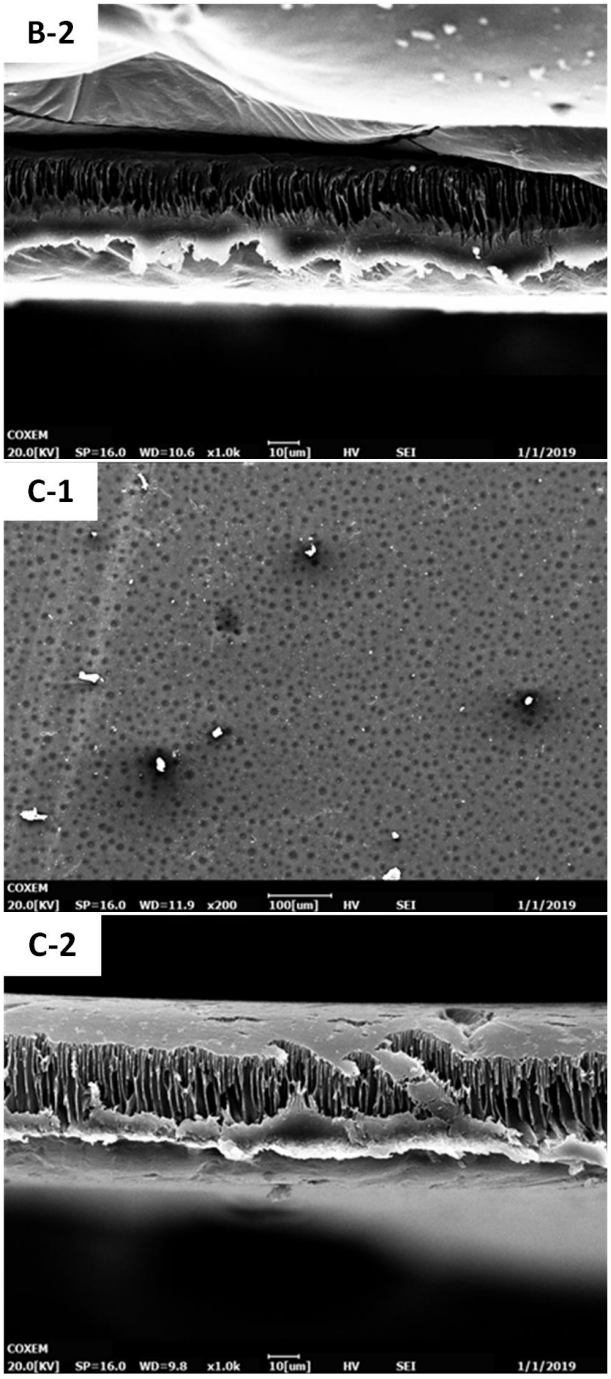


**Figure 6** Surface and Cross Section Morphology of Membrane (A) Neat PES Membrane (B) 1.5%wt of Nano ZnO PES Membrane (C) Nano ZnO-PES Membrane with UV 1 minutes, the code 1 and 2 indicate surface and cross-section images, respectively

## Water Contact Angle Measurement of Membranes Surface

Contact angle analysis was performed by using Race Angle Meter with ion-free distilled water at 25°C. This analysis aimed to determine whether the membrane was hydrophilic or hydrophobic. The results are shown in Table 3.

Based on Table 3. PES membranes with compositions 17, 18, and 20 wt% have contact angles of 65.5, 62.67, and 62.17°, respectively. The data indicate that PES membranes were hydrophilic. The addition of nano ZnO as a non-polymeric compound improved the hydrophilicity of the PES membrane as shown lower contact angle of the PES-ZnO membrane than that of the PES membrane. This fact is due to the larger surface area of the nano ZnO particles, which causes nano ZnO can easily absorb the hydrophilic (-OH) hydroxyl groups [21]. In addition, the increasing hydroxyl groups in the membrane was also caused by free electrons contained in nano ZnO [29]. Like-wise with the use of UV irradiation carried can improve the hydrophilicity of the membrane as indicated by a decrease in the contact angle produced after UV radiation on the membrane. This phenomenon is the result of the production of polar functional groups on membrane surfaces upon UV irradiation [30].

**Table 3** Water contact angle measurement results

| Membrane | Detailed formula | Average |
|---|---|---|
| M1 | PES 17% | 65.5 ± 1 |
| M2 | PES 18% | 62.7 ± 1 |
| M3 | PES 20% | 62.2 ± 1.5 |
| M4 | PES 17% - ZnO 1.5% | 60 ± 1.3 |
| M5 | PES 17% - ZnO 2% | 53.5 ± 1 |
| M6 | PES 17% - ZnO 2.5% | 52.8 ± 0.8 |
| M7 | PES 17% - ZnO 1.5% - UV 0.5 min | 52.8 ± 0.8 |
| M8 | PES 17% - ZnO 1.5% - UV 1 min | 51.5 ± 0.5 |

## 4.0 CONCLUSION

Nano ZnO addition and UV treatment on membranes significantly influence the biodiesel purification process, especially by reducing the glycerol contents. The nano ZnO particles addition increases glycerol rejection. For UV Irradiation, flux profile and glycerol rejection vary as a function of UV irradiation times. The best biodiesel purification performance was achieved using membranes which composed of PES 18 wt%, ZnO 1.5 wt%, and UV irradiated for 1 minute

## Acknowledgement

This research was financially supported by Diponegoro University through the research scheme of International Publication Research (RPI). We would thank to waste treatment laboratory of Chemical Engineering Department of Diponegoro University for the facilities support during the research

## References

[1] Dudley, B. 2018. BP Statistical Review of World Energy. BP Statistical Review, London, UK, accessed Dec, 6, 2019. https://www.bp.com/content/dam/bp/business-sites/en/global/corporate/pdfs/news-and-insights/speeches/bp-stats-review-2019-bob-dudley-speech.pdf.

[2] Brennan, L., & Owende, P. 2010. Biofuels from Microalgae - A Review of Technologies for Production, Processing, and Extraction of Biofuels and Co-products. *Renewable Sustain Energy*. 14(2): 557-577. DOI: https://doi.org/10.1016/j.rser.2009.10.009.

[3] Makertihartha, I. G. B. N., Khoiruddin, K., Nabu, E. B. P., Aryanti, P. T. P., & Wenten, I. G. 2019. Simultaneous Methyl Ester Production and Carotene Recovery from Crude Palm Oil Using Membrane Reactor. *Jurnal Teknologi*. 81(2): 27-38. DOI: https://doi.org/10.11113/jt.v81.12539.

[4] Medeiros, A. M., Santos, Ê. R., Azevedo, S. H., Jesus, A. A., Oliveira, H. N., & Sousa, E. M. 2018. Chemical Interesterification of Cotton Oil with Methyl Acetate Assisted by Ultrasound for Biodiesel Production. Brazilian *Journal of Chemical Engineering*. 35(3): 1005-1018. DOI: http://dx.doi.org/10.1590/0104-6632.20180353s20170001.

[5] Ma, F., & Hanna, M. A. 1999. Biodiesel Production; A Review. *Bioresource Technology*. 70(1): 1-15. DOI: https://doi.org/10.1016/S0960-8524(99)00025-5.

[6] Alves, M., Cavalcanti, I., Resende, M., Carsodo, V., & Reis, I. 2016. Biodiesel Dry Purification with Sugarcane Bagasse. *Industrial Corps and Products*. 89: 119-127. DOI: https://doi.org/10.1016/j.indcrop.2016.05.005.

[7] Wall, J., Gerpen, J. V., & Thompson, J. 2011. Soap and Glycerin Removal from Biodiesel using Waterless Processes. *Transaction of the Asabe*. 54(2): 535-541. DOI: https://doi.org/10.13031/2013.36456

[8] Escorsim, A., Cordeiro, C., Ramos, L., Ndiaye, P., Kanda, L., & Corazza, M. 2015. Assessment of Biodiesel Purification Using CO2 at High Pressures. *Journal of Supercritical Fluids*. 96: 68-76. DOI: https://doi.org/10.1016/j.supflu.2014.08.013.

[9] Alves, M., Nascimento, S., Pereira, I., Martins, M., Cardoso, V., & Reis, M. 2013. Biodiesel Purification Using Micro and Ultrafiltration Membranes. *Renewable Energy*. 58: 15-20. DOI: https://doi.org/10.1016/j.renene.2013.02.035.

[10] Atadashi, I. M. 2015. Purification of Crude Biodiesel using Dry Washing. *Alexandria Engineering Journal*. 54(4): 1265-1272. DOI: https://doi.org/10.1016/j.aej.2015.08.005.

[11] Lai, G. S., Lau, W. J., Goh, P. S., Tan, Y. H., Ismail, A. F., Zaik, U., Basri, H., & Gohari, R. J. 2017. Preparation and Characterization of Superhydrophilic Nanocomposite Ultrafiltration Membranes for Treatment of Highly Concentrated Oil-in-water Emulsion. *Jurnal Teknologi*. 79(1-2): 53-58. DOI: https://doi.org/10.11113/jt.v79.10437.

[12] Shen, L., Bian, X., Lu, X., Shi, L., Liu, Z., Chen, L., & Fan, K. 2012. Preparation and Characterization of ZnO/polyethersulfone (PES) Hybrid Membranes. *Desalinaion*. 293: 21-29. DOI: https://doi.org/10.1016/j.desal.2012.02.019.

[13] Pisarello, M. L., Dalla Costa, B. O., Veizaga, N. S., & Querini, C. A. 2010. Volumetric Method for Free and Total Glycerin Determination in Biodiesel. *Industrial & Engineering Chemistry Research*. 49(19): 8935-8941. DOI: https://doi.org/10.1021/ie100725f

[14] Liao, C., Yu, P., Zhao, J., Wang, L., & Luo, Y. 2011. Preparation and Characterization of NaY/PVDF Hybrid Ultrafiltration Membranes Containing Silver Ions as Antibacterial Materials. *Desalination*. 272(1-3): 59-65. DOI: https://doi.org/10.1016/j.desal.2010.12.048.

[15] Panda, Swapna Rekha; De,Sirshend. 2014. Preparation Characterization and Performance of ZnCl2 Incorporated

Polysulfone (PSf)/polyethylene Glycol(PEG) Blend Low Pressure Nanofiltration Membranes. *Desalination.* 347: 52-65. DOI: https://doi.org/10.1016/j.desal.2014.05.030.

[16] Nasrollahi, N., Vatanpour, V., Aber, S., & Mahmoodi, N. M. 2018. Preparation and Characterization of a Novel Polyethersulfone (PES) Ultrafiltration Membrane Modified with a CuO/ZnO Nanocomposite to Improve Permeability and Antifouling Properties. *Separation and Purification Technology.* 192: 369-382. DOI: https://doi.org/10.1016/j.seppur.2017.10.034.

[17] Kusworo, T. D., Qudratun, & Utomo, D. P. 2017. Performance Evaluation of Double Stage Process Using Nano Hybrid PES/SiO2-PES Membrane and PES/ZnO-PES Membranes for Oily Waste Water Treatment to Clean Water. *Journal of Enviromental Chemical Engineering. 5*: 6077-6086. DOI: https://doi.org/10.1016/j.jece.2017.11.044.

[18] Porter, M. C. 1999. *Handbook of Industrial Membrane Technology*. Noyes Publicaions: New Jersey.

[19] Mulder, M. 1996. *Basic Principles of Membrane Technology*. Kluwer Academic Publishers: Netherlands.

[20] Lin, J., Ye, W., Zhong, K., Shen, J., Jullok, N., Sotto, A., & Bruggen, B. 2016. Enhancement of PES Membrane Doped by Monodisperse Stober Silica for Water Treatment. *Chemical Engineering and Processing: Process Intensification.* 107: 194-205. DOI: https://doi.org/10.1016/j.cep.2015.03.011

[21] Shen, Y., & Lua, A. 2012. Preparation And Characterization Ofmixed Matrix Membranes based on PVDF and Three Inorganicfillers (Fumed Nonporous Silica, Zeolite 4A and Mesoporous MCM-41) for Gas Separation. *Chemical Engineering Journal.* 192: 201-210. DOI: https://doi.org/10.1016/j.cej.2012.03.066.

[22] Nikooe, N., & Saljoughi, E. 2017. Preparation and Characterization of Novel PVDF Nanofiltration Membranes with Hydrophilic Property for Filtration of Dye Aqueous Solution. *Applied Surface Science*. 413: 41-49. DOI: https://doi.org/10.1016/j.apsusc.2017.04.029.

[23] Chen, X., Wu, S., & Zhou, J. 2013. Influence of Porosity on Compressive and Tensile Strength of Cement Mortar. *Construction and Building Material.* 40: 869-874. DOI: https://doi.org/10.1016/j.conbuildmat.2012.11.072

[24] Kusworo, T. D., Soetrisnanto, D., Aryanti, N., Utomo, D. P., Qudratun, Tambunan, V. D., & Simanjuntak, N. R. 2018. Evaluation of Integrated Modifies Nanohybrid Polyethersulfone-ZnO Membrane with Single Stage and Double Stage System For Produced Water Treatment Into Clean Water. *Journal of Water Process Engineering*. 23: 239-249. DOI: https://doi.org/10.1016/j.jwpe.2018.04.002.

[25] Rajabi, H., Ghaemi, N., Madaeni, S. S., Daraei, P., Astinchap, B., Zinadini, S., & Razavizadeh, S. H. 2015. Nano-ZnO Embedded Mixed Matrix Polyethersulfone (PES) Membrane: Influence of Nanofiller Shape on Characterization and Fouling Resistance. *Applied Surface Science.* 349: 2-44. DOI: https://doi.org/10.1016/j.apsusc.2015.04.214

[26] Kusworo, T. D., Aryanti, N., Anggita, R. A., Setyorini, T. A. D., & Utomo, D. P. 2017. Surface Modification and Performance Enhancement of Polyethersulfone (PES) Membrane Using Combination of Ultra Violet Irradiation and Thermal Annealing for Produced Water Treatment. *Journal of Environmental Science and Technology*. 10(1): 35-43. DOI: https://doi.org/ 10.3923/jest.2017.35.43.

[27] Pavia, D., Lampman, G., & Kriz, G. 2001. *Introduction To Spectroscopy: A Guide for Students of Organic Chemistry*. Department of Chemistry Western Washington University, Washington.

[28] Susanto, H., & Ulbricht, M. 2007. Photografted Thin Polymer Hydrogel Layers on PES Ultrafiltration Membranes: Characterization, Stability, and Influence on Separation Performance. *Langmuir*. 23(14): 7818-7830. DOI: https://doi.org/10.1021/la700579x.

[29] Kusworo, T. D., Aryanti, N., & Utomo, D. P. 2018. Oilfield Produced Water Treatment to Clean Water Using Integrated Activated Carbon-bentonite Adsorbent and Double Stages Membrane Process. *Chemical Engineering Journal*. 347: 462-471. DOI: https://doi.org/10.1016/j.cej.2018.04.136.

[30] Konruang, S., Chittrakarn, T., & Sirijarukul, S. 2014. Surface Modification of Asymmetric Polysulfone Membrane by UV Irradiation. *Jurnal Teknologi* (Sciences & Engineering). 70(2): 55-60. DOI: https://doi.org/10.11113/jt.v70.3435.